Electronic Supplementary Information

Sulfonic acid-Functionalized Organic Knitted Porous Polyaromatic Microspheres as Heterogeneous Catalysts for Biodiesel Production

*Anuraj Varyambath, Mi-Ra Kim, and Il Kim**

BK21 PLUS Center for Advanced Chemical Technology, Department of Polymer Science and Engineering, Pusan National University, Busan 609-735, Republic of Korea

*Corresponding author: ilkim@pusan.ac.kr

Table S1 The physical properties of Organic Knitted Porous Polymers

Name of the catalyst	S_{BET} (m^2/g)	V_{micro} (cm^3/g)	Pore diameter (nm)
OPP-1	595	0.5247	0.86
OPP-2	520	0.5024	0.72
OPP-3	458	0.4982	0.80

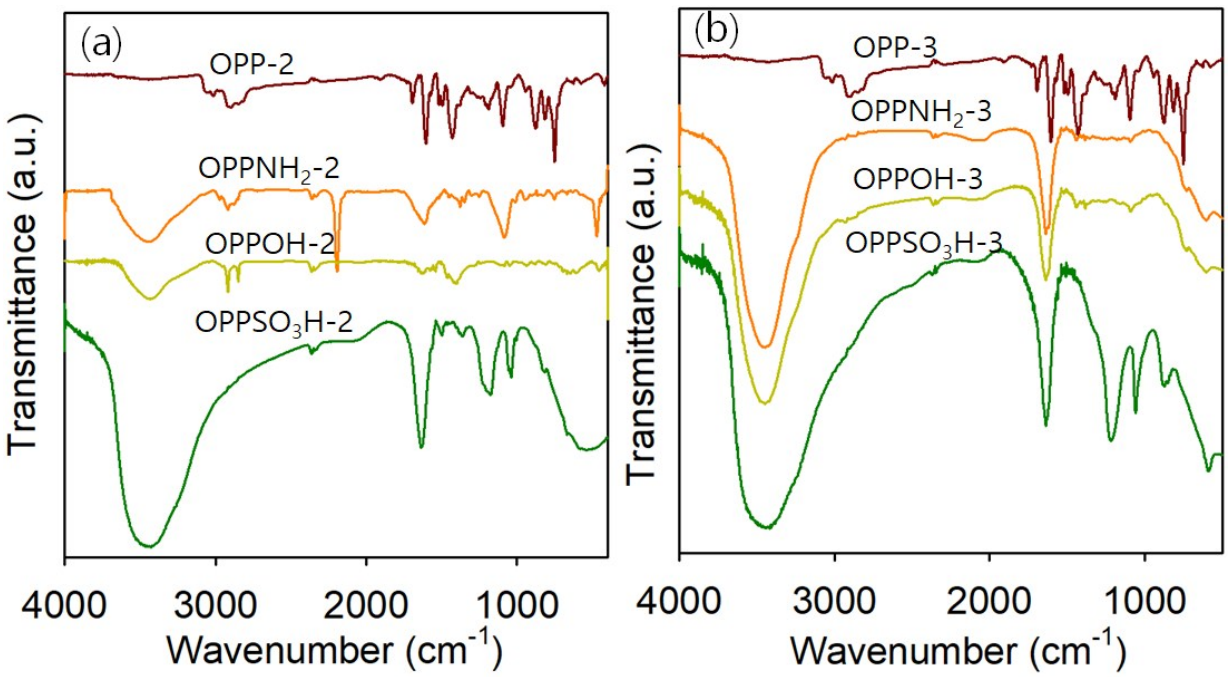

Fig. S1. FTIR spectra of OPP-2 (a) and OPP-3 (b), and their functionalized products.

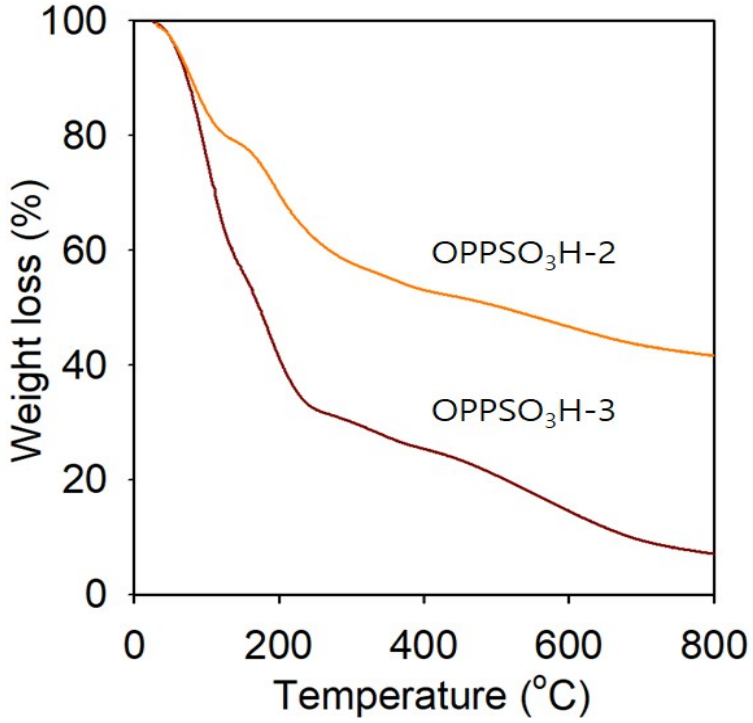

Fig. S2. TGA curves of $OPPSO_3H$-2 and $OPPSO_3H$-3.

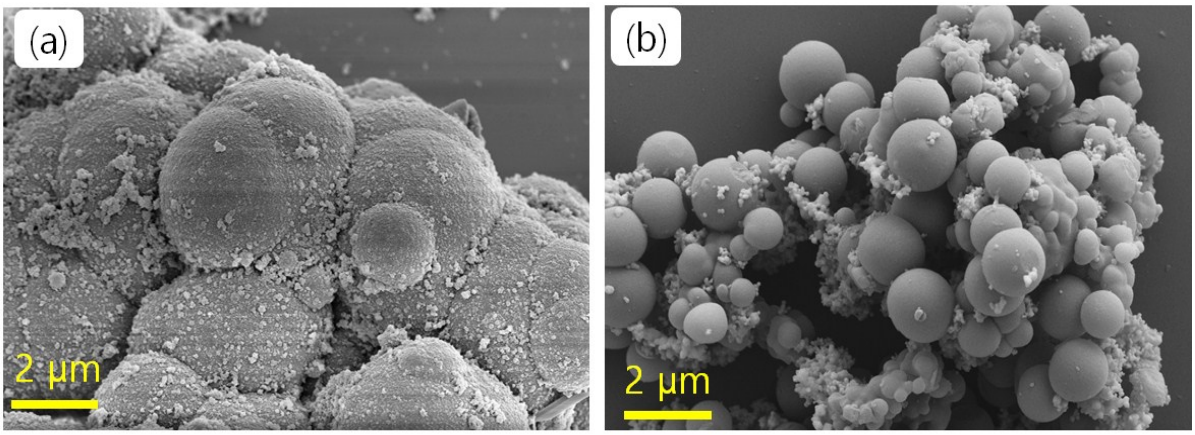

Fig. S3. FESEM images of $OPPSO_3H$-2 (a) and $OPPSO_3H$-3 (b).

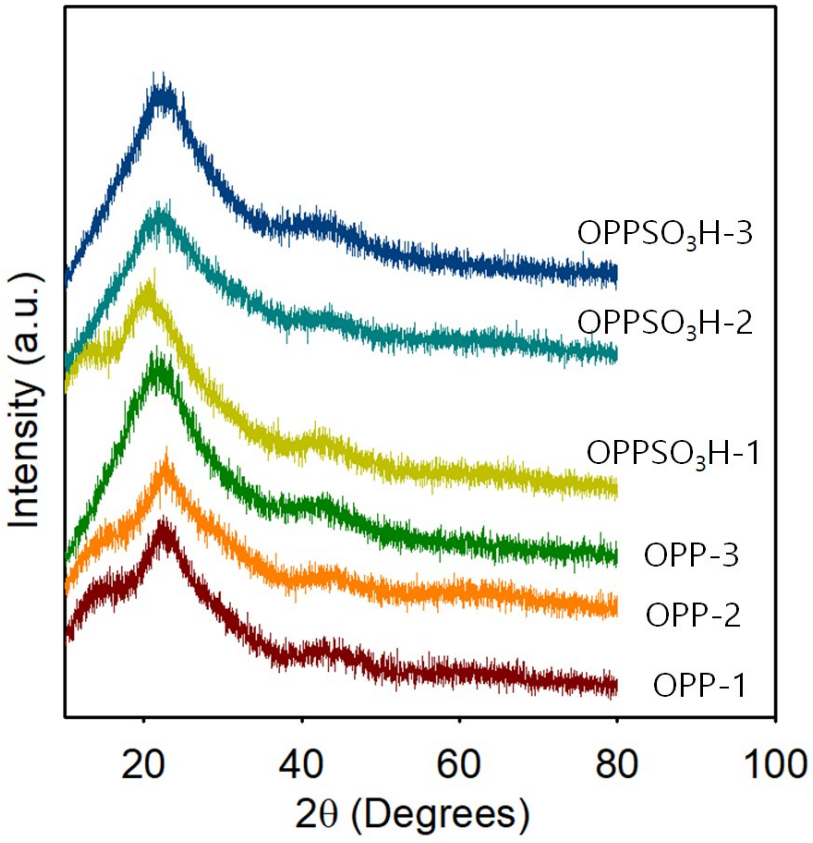

Fig. S4. XRD patterns of OPPs and $OPPSO_3Hs$.

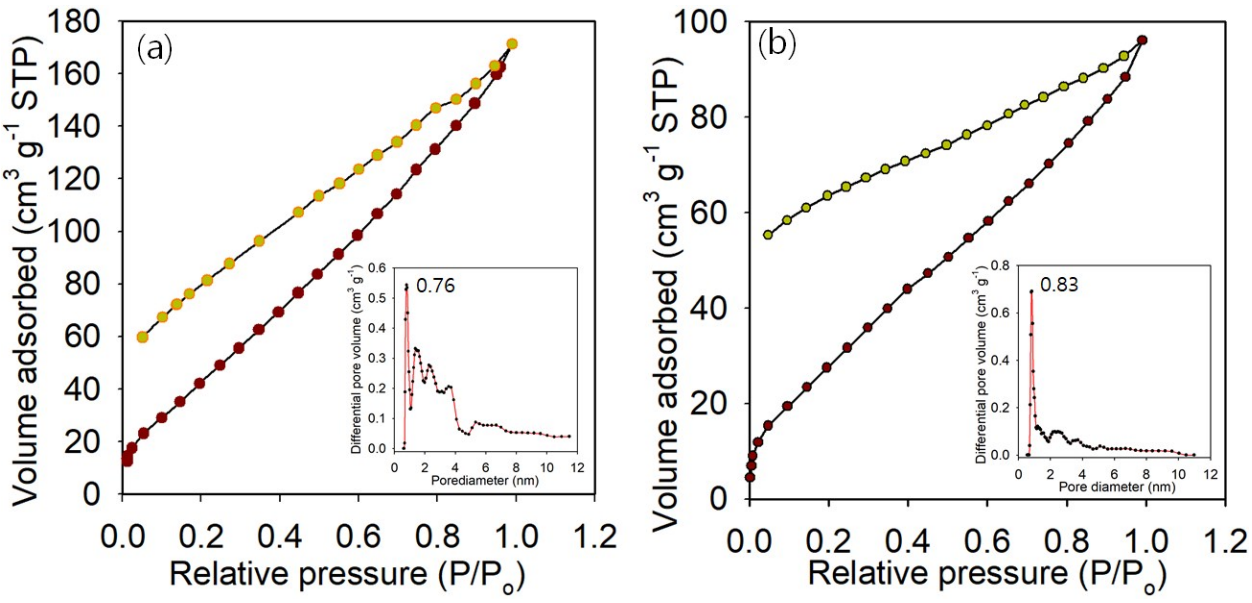

Fig. S5. N_2 adsorption/desorption isotherm and corresponding pore size distribution curves (shown in inset) calculated from NLDFT method of $OPPSO_3H$-2 (a) and $OPPSO_3H$-3(b).

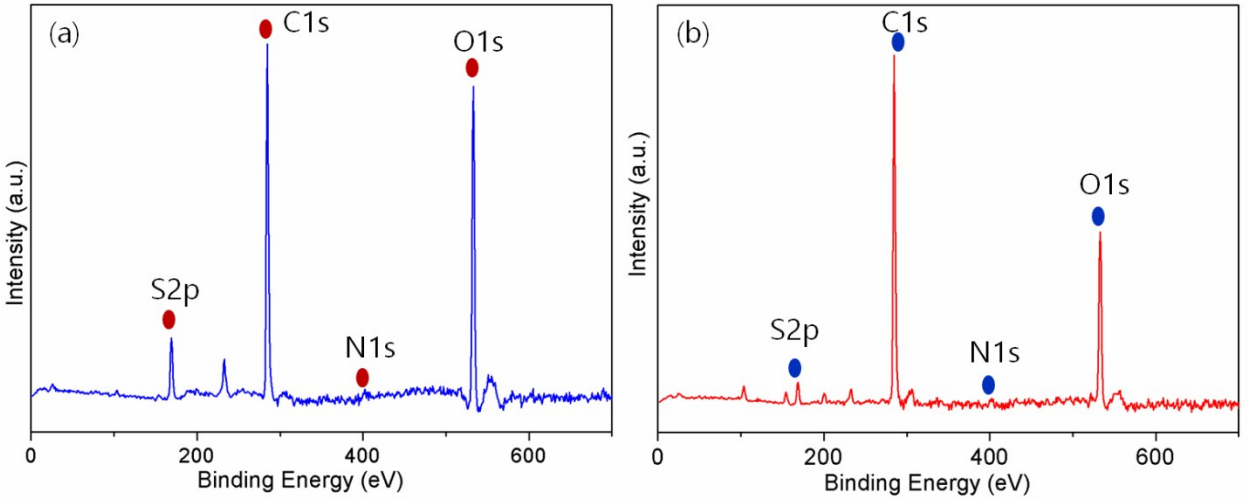

Fig. S6. Wide scan XPS spectra of $OPPSO_3H$-2 (a) and , $OPPSO_3H$-3 (b).

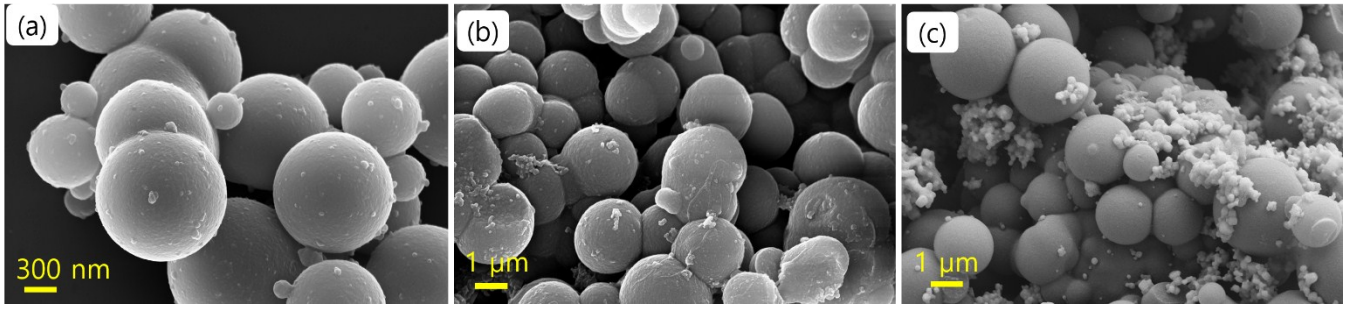

Fig. S7. FESEM images of $OPPSO_3H$-1 (a) $OPPSO_3H$-2 (b) and $OPPSO_3H$-3 (c) after catalytic reactions.

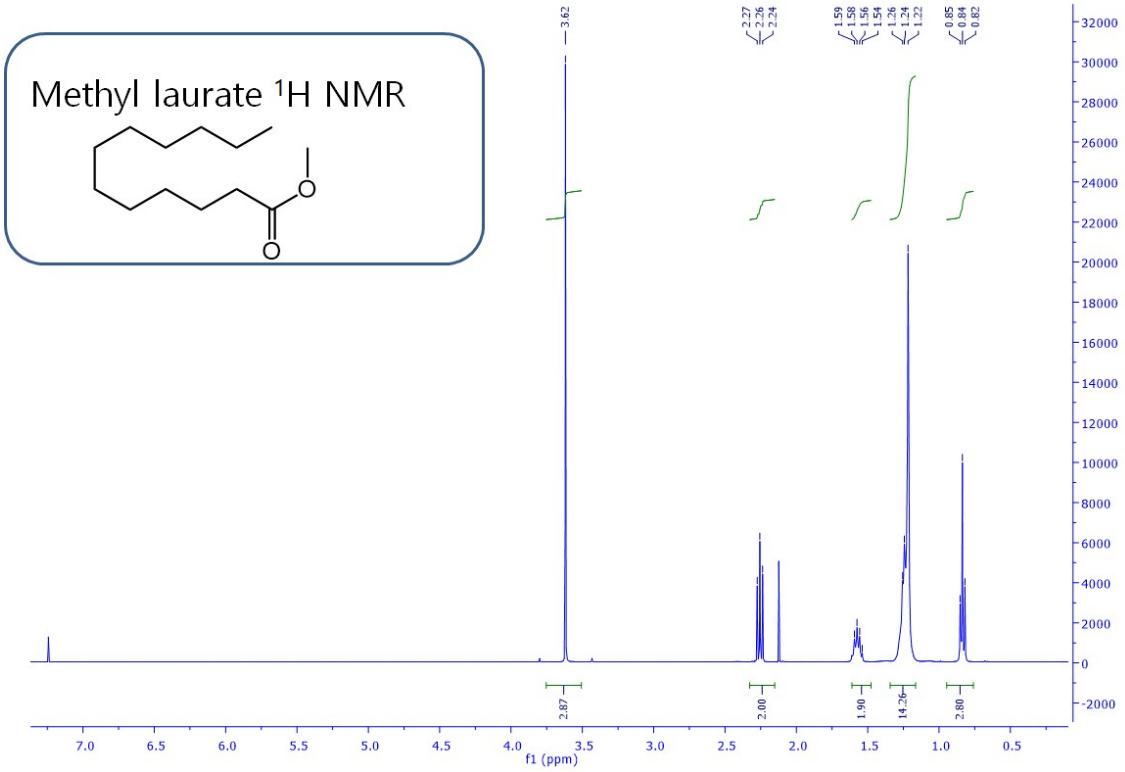

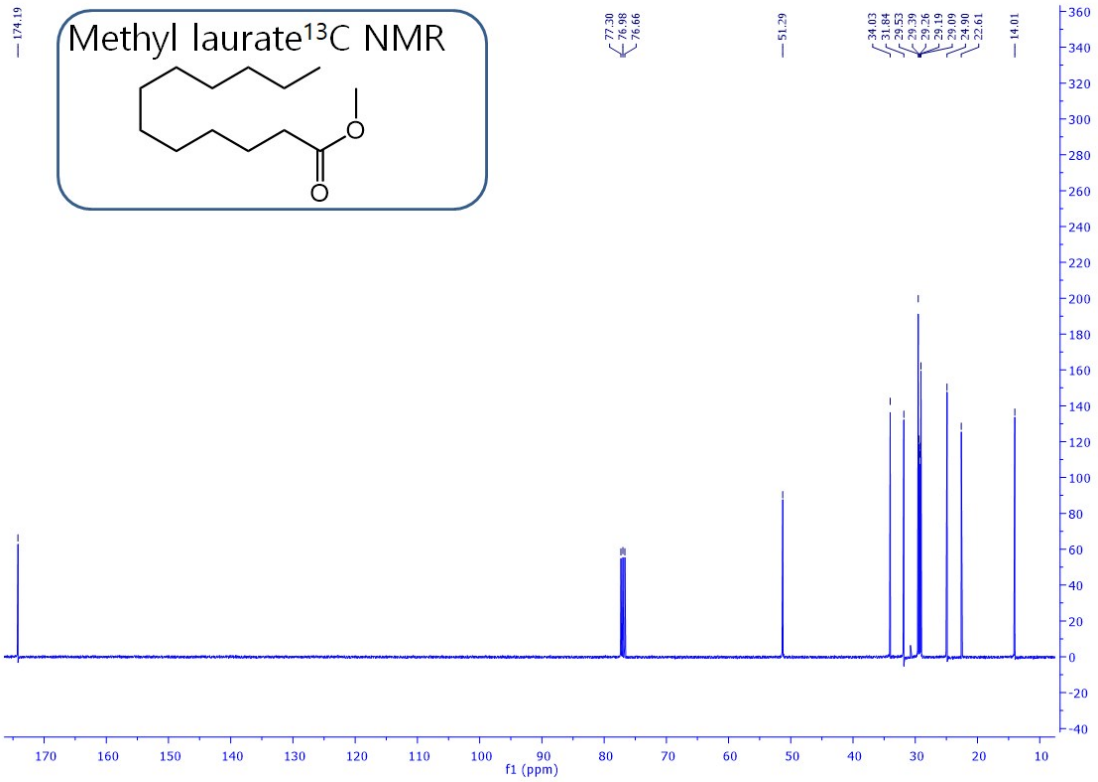

Fig. S8. ^{1}H and ^{13} C NMR spectra of methyl laurate obtained by esterification using $OPPSO_3H$-1.

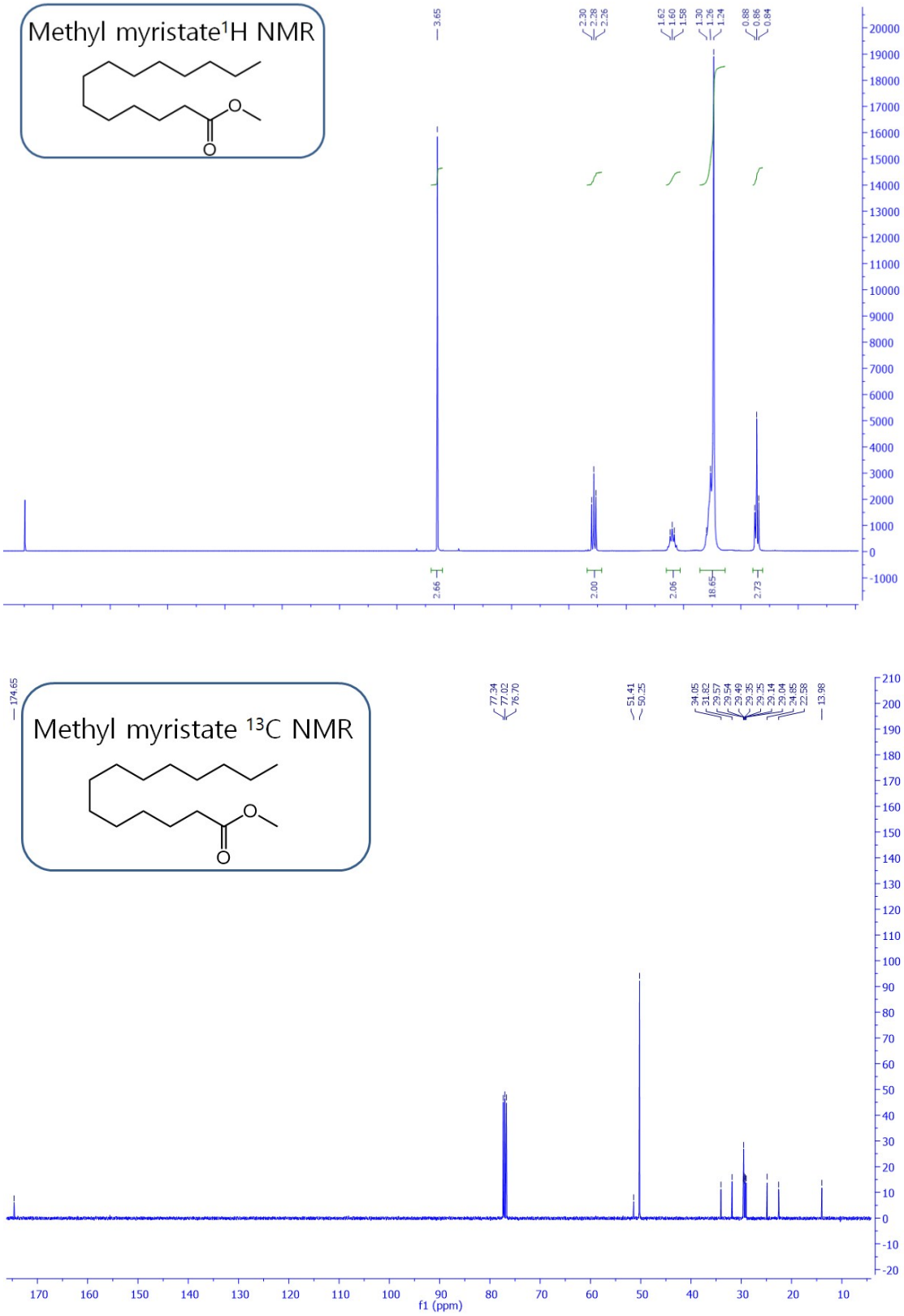

Fig. S9. ^{1}H and ^{13} C NMR spectra of methyl myristate obtained by esterification using $OPPSO_3H$-1.

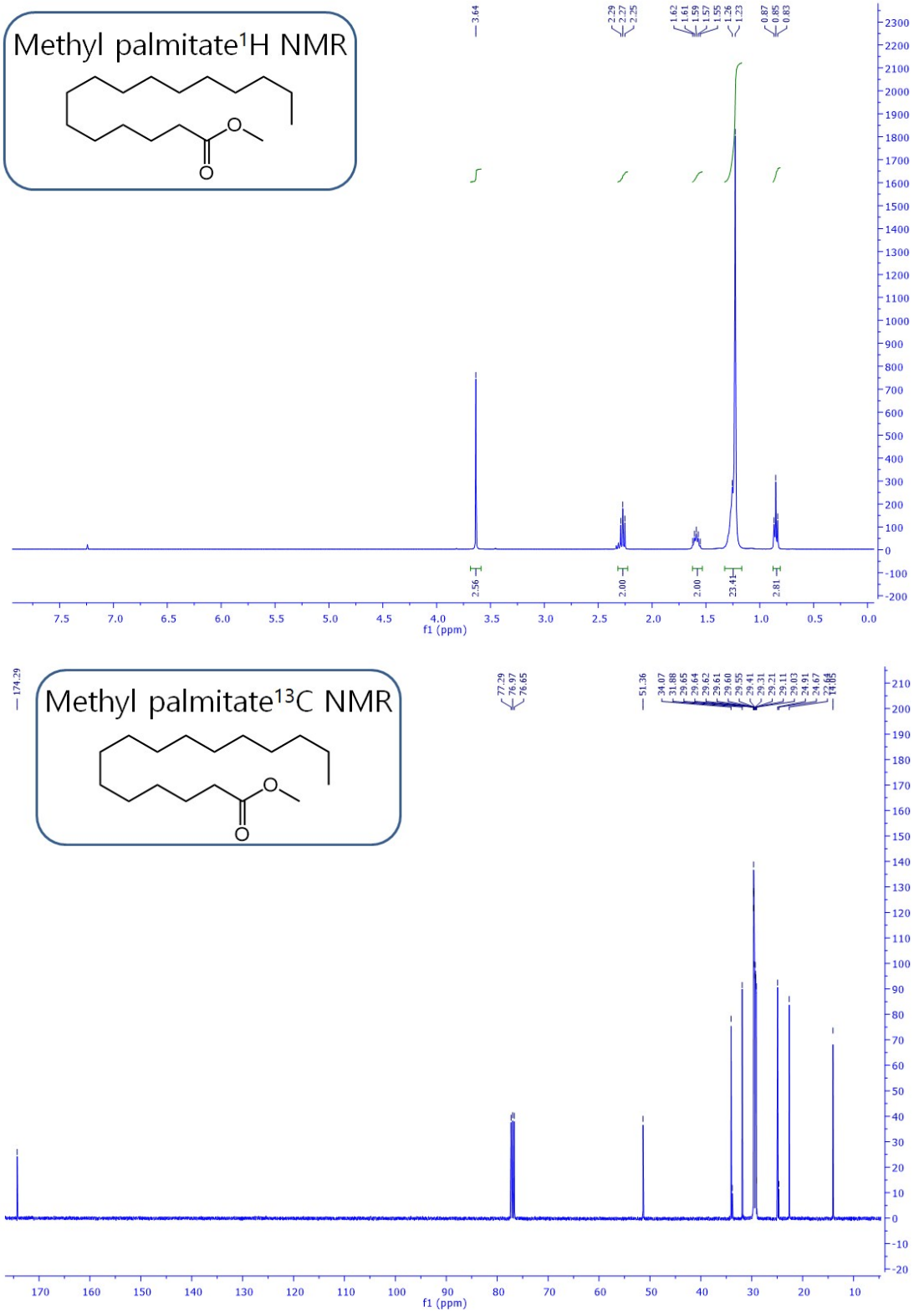

Fig. S10. ^{1}H and ^{13} C NMR spectra of methyl palmitate obtained by esterification using $OPPSO_3H$-1.

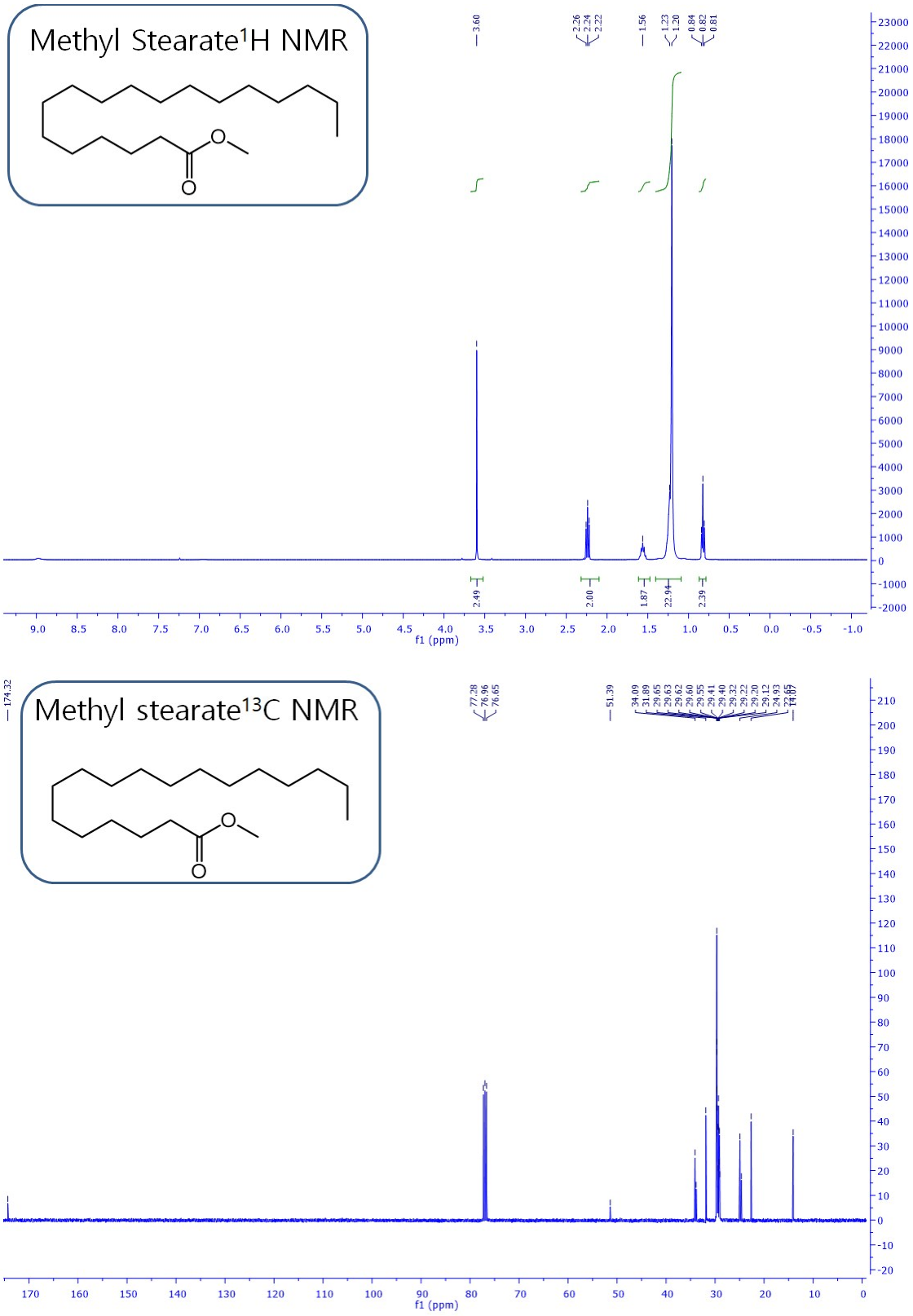

Fig. S11. [1]H and [13] C NMR spectra of methyl stearate obtained by esterification using $OPPSO_3H$-1.

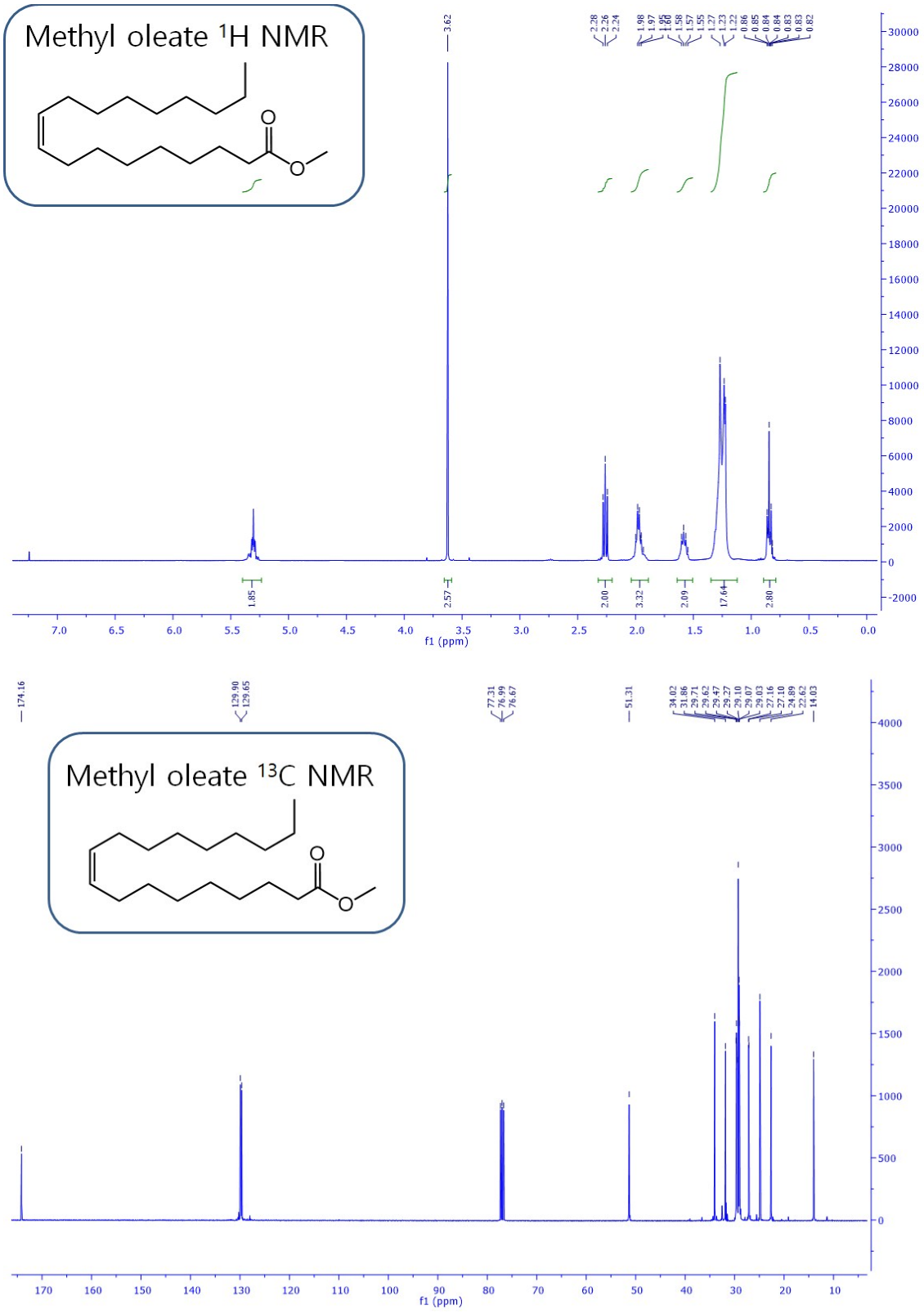

Fig. S12. [1]H and [13] C NMR spectra of methyl oleate obtained by esterification using $OPPSO_3H$-1.

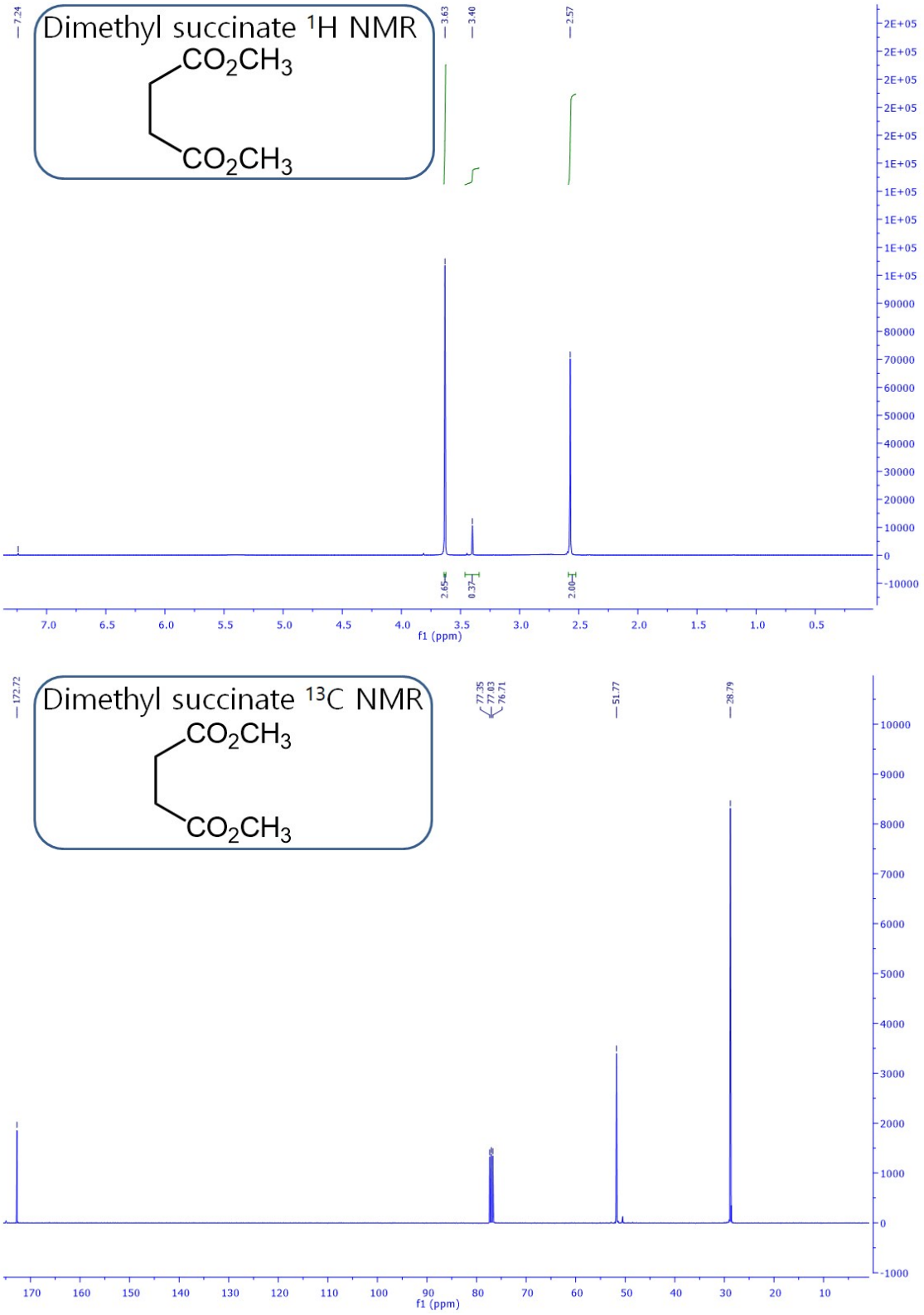

Fig. S13. [1]H and [13] C NMR spectra of dimethyl succinate obtained by esterification using $OPPSO_3H$-1.

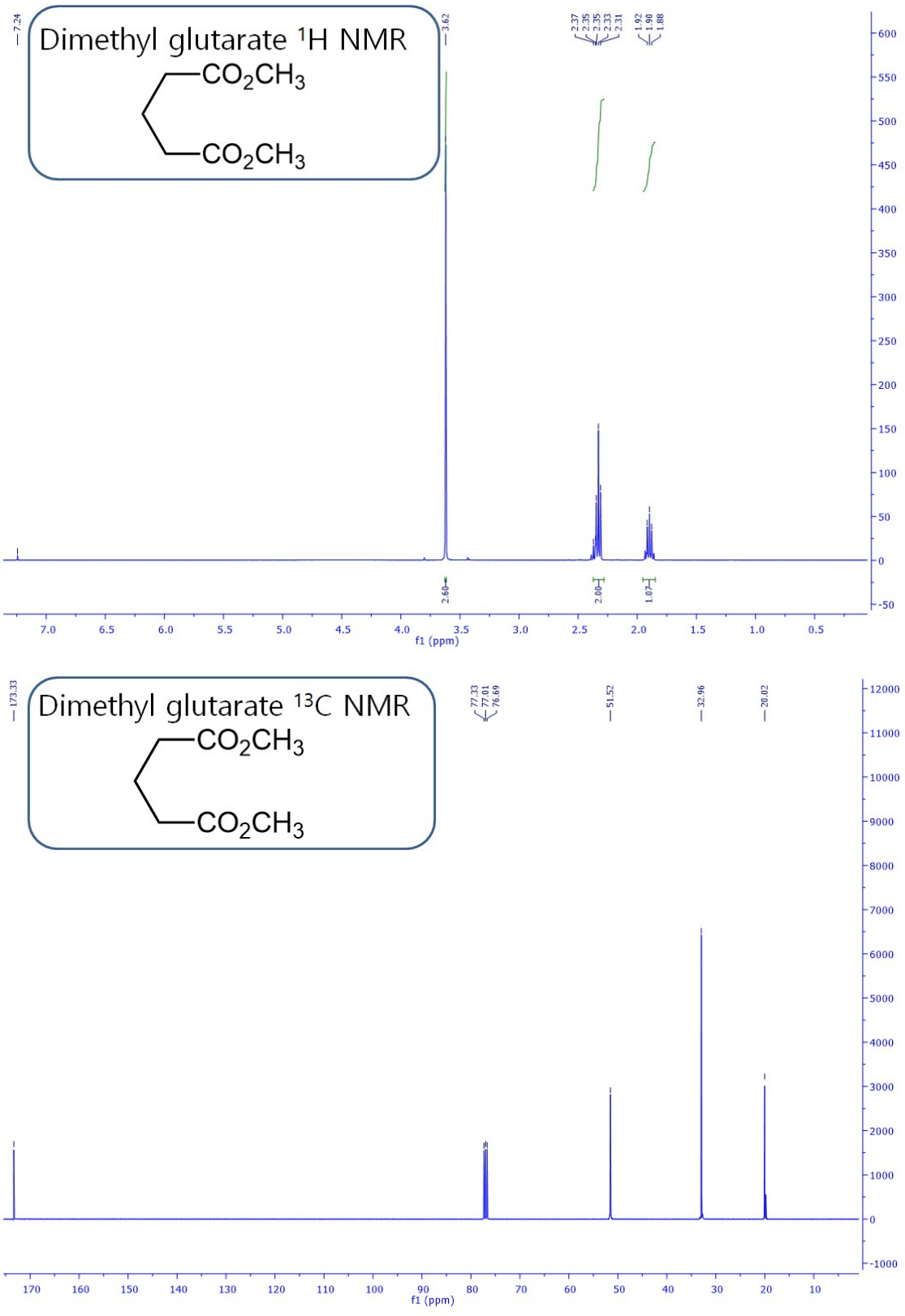

Fig. S14. [1]H and [13] C NMR spectra of dimethyl glutarate obtained by esterification using $OPPSO_3H$-1.

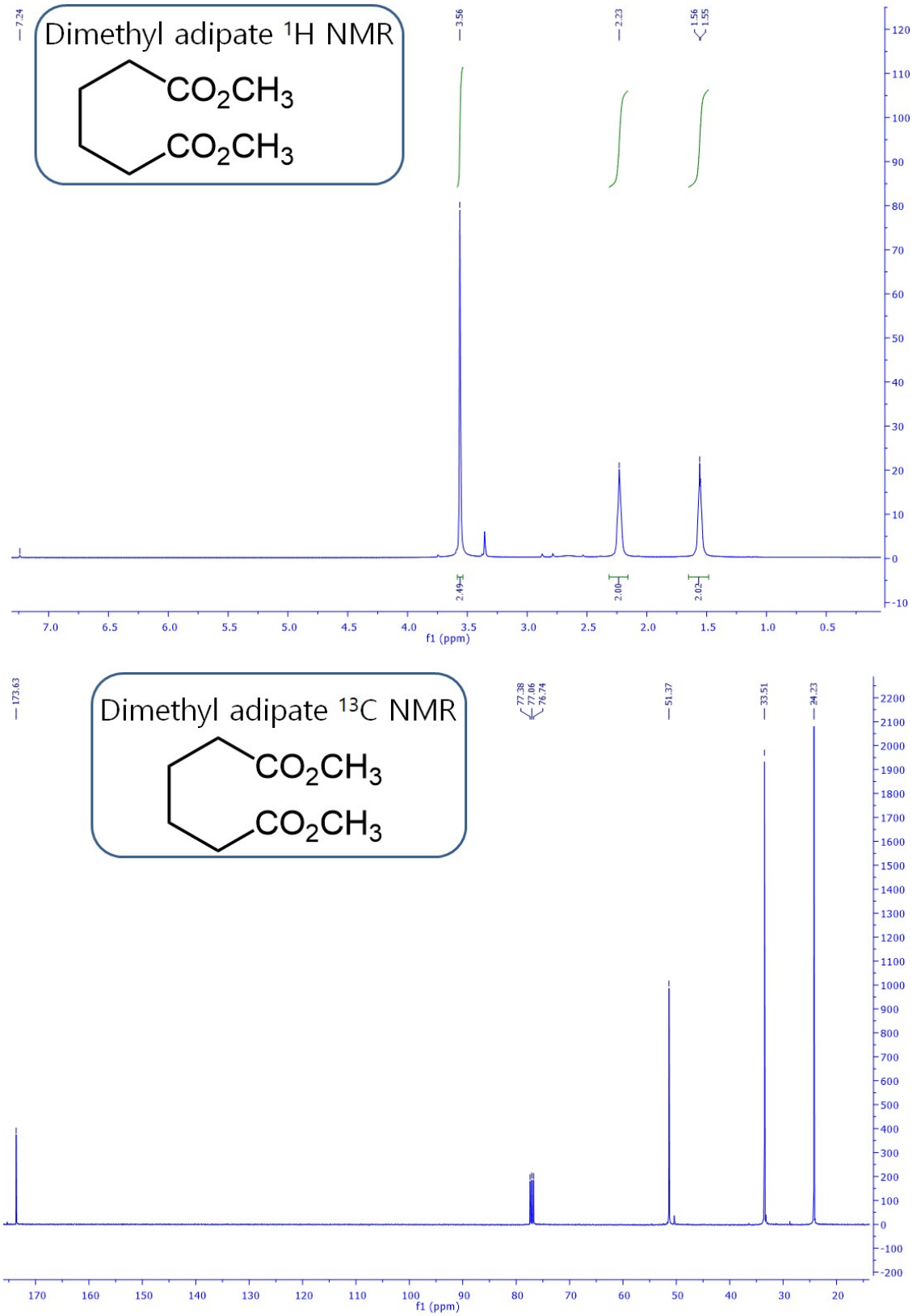

Fig. S15. [1]H and [13] C NMR spectra of dimethyl adipate obtained by esterification using $OPPSO_3H$-1.

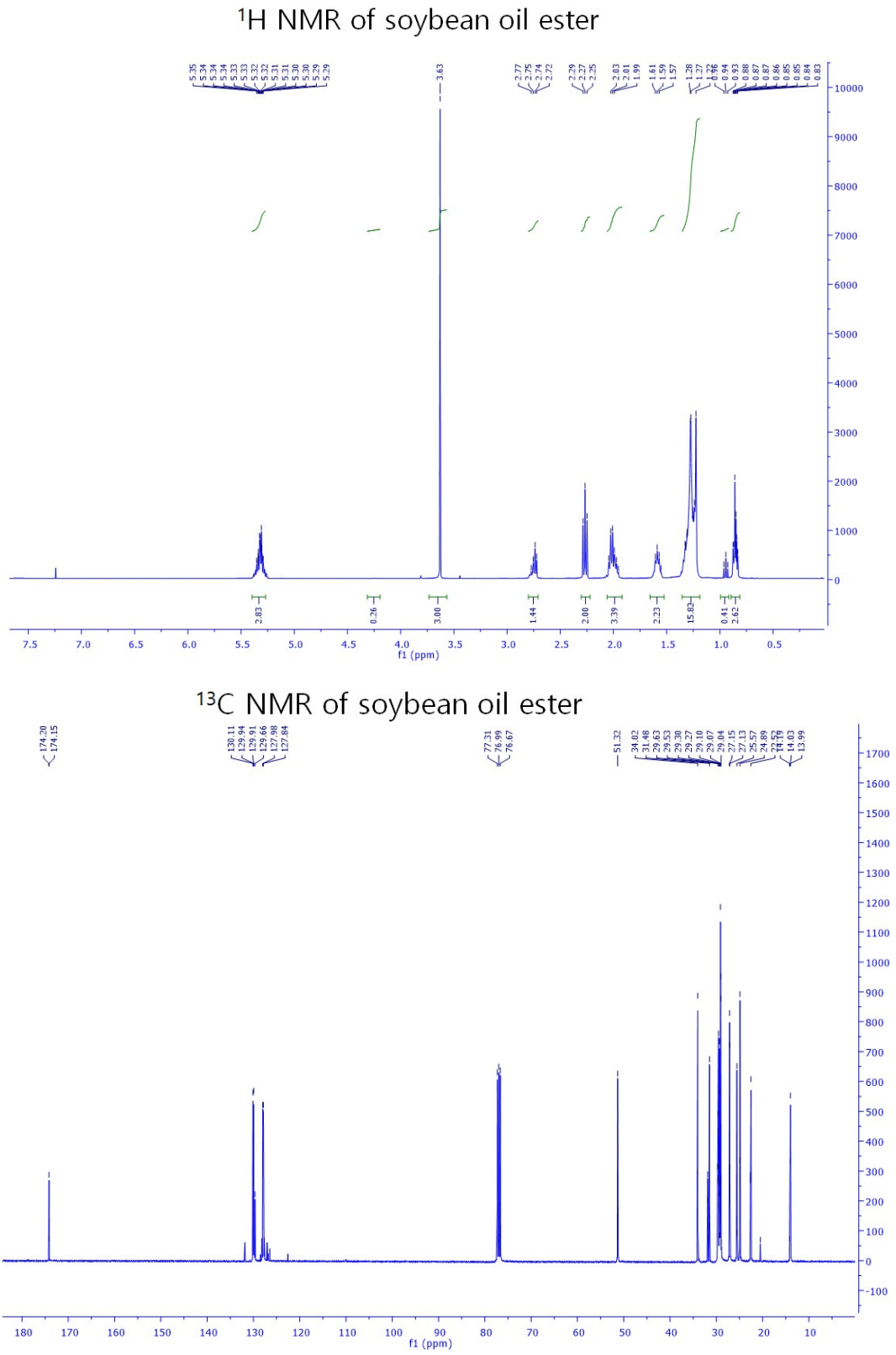

Fig. S16. [1]H and [13] C NMR spectra of soybean oil ester obtained by transesterification using $OPPSO_3H$-1.

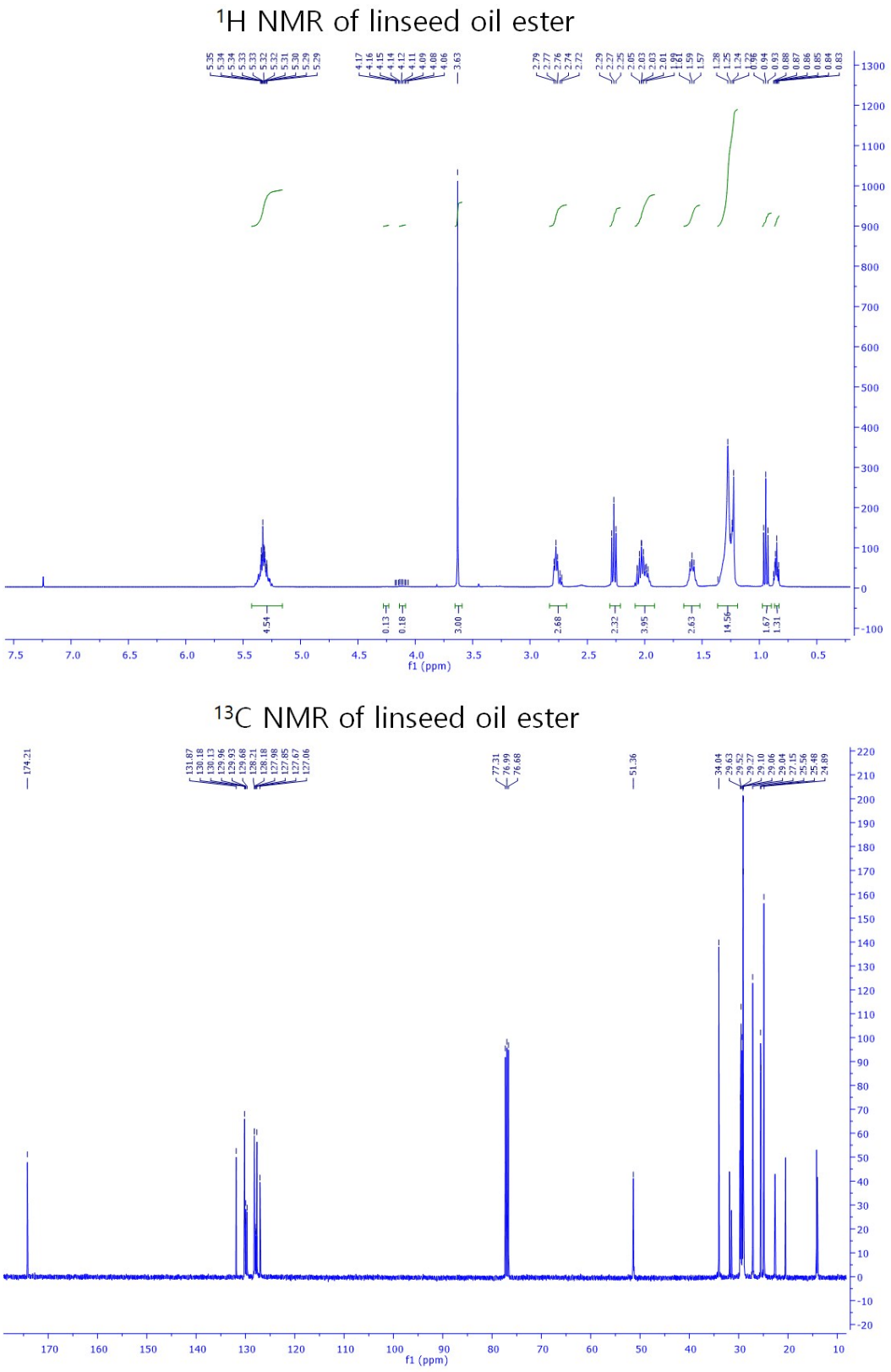

Fig. S17. ^{1}H and ^{13} C NMR spectra of linseed oil ester obtained by transesterification using $OPPSO_3H$-1.

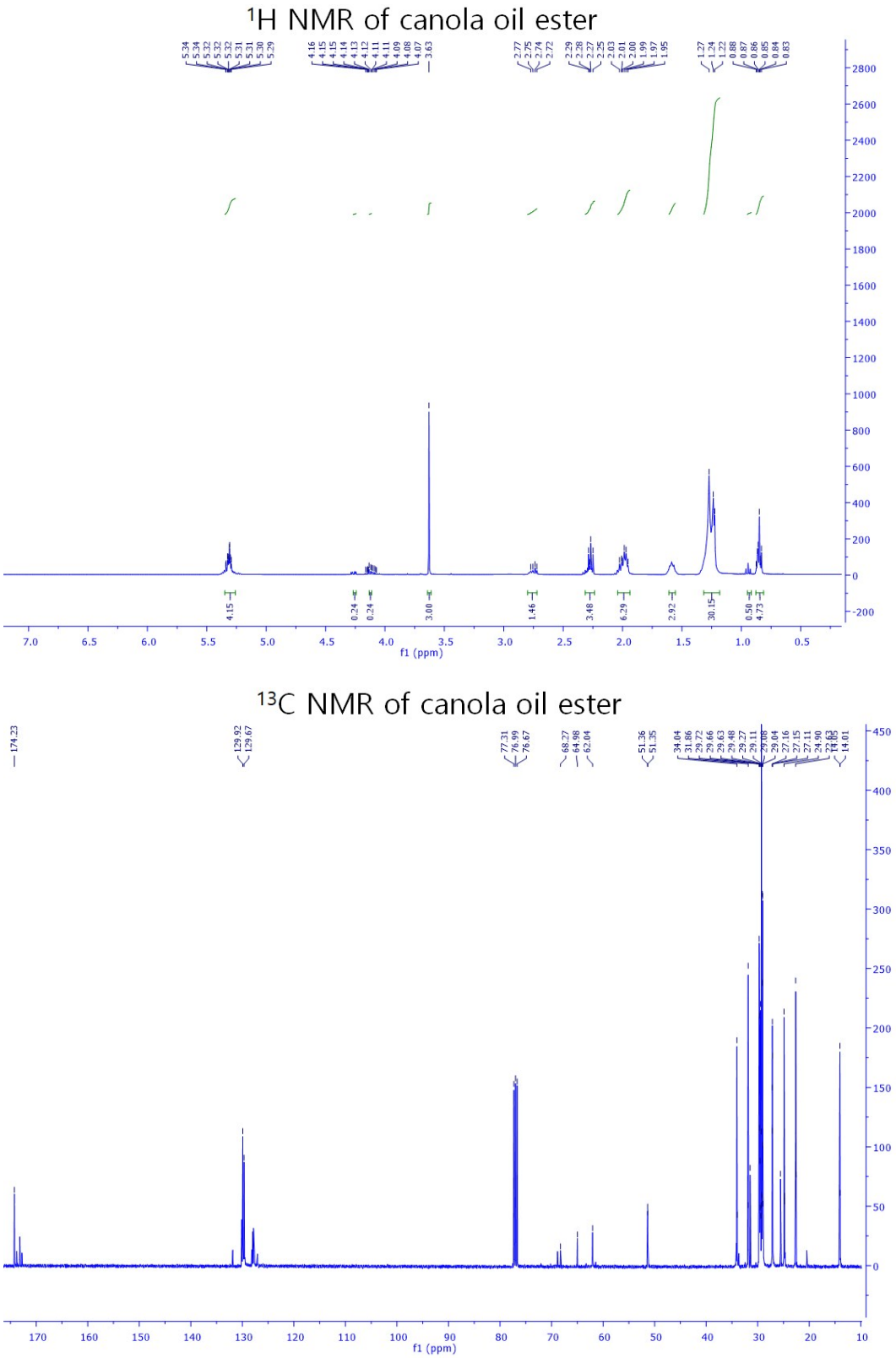

Fig. S18. [1]H and [13] C NMR spectra of canola oil ester obtained by transesterification using $OPPSO_3H$-1.

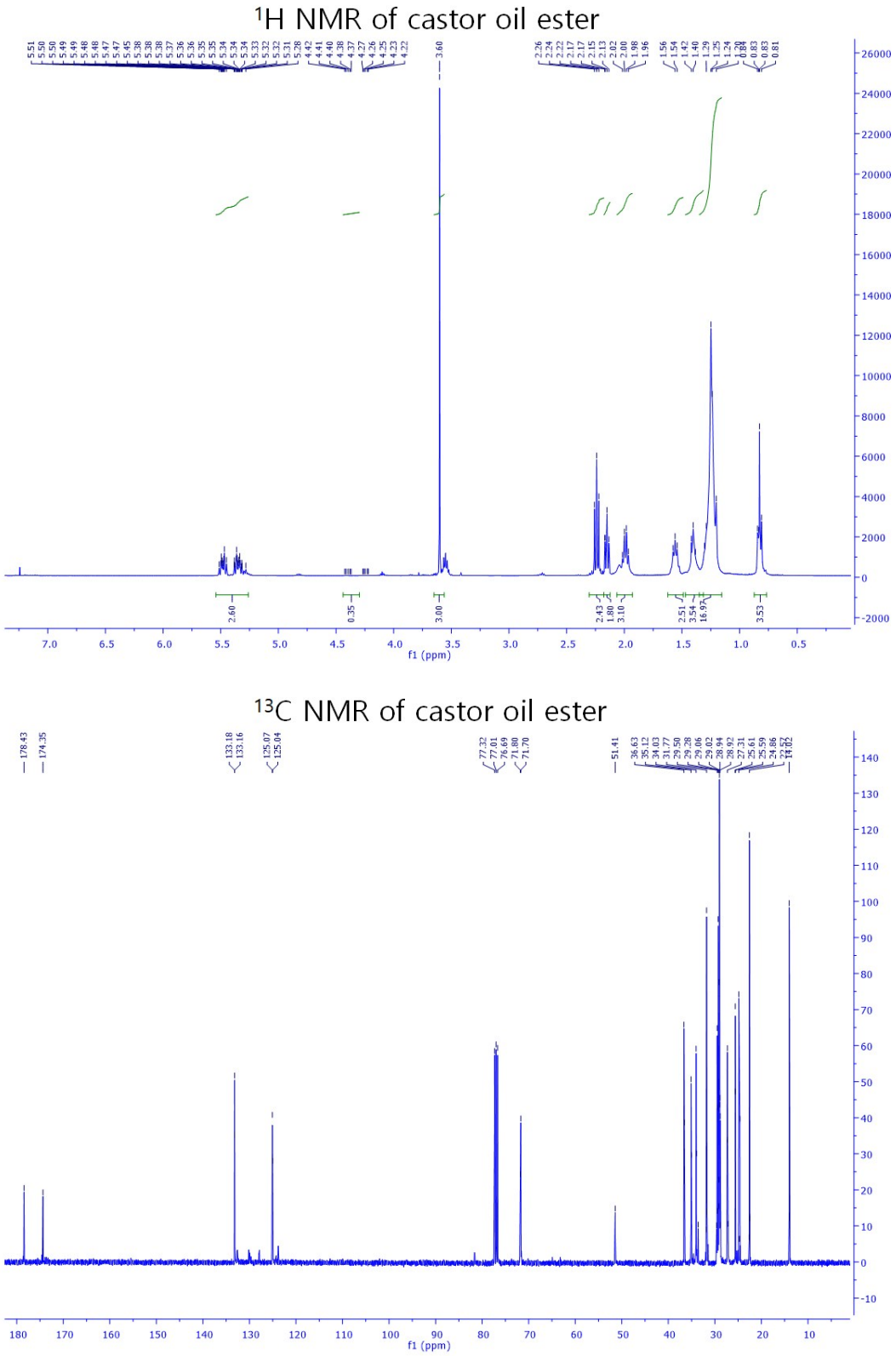

Fig. S19. ^{1}H and ^{13} C NMR spectra of castor oil ester obtained by transesterification using $OPPSO_3H$-1.

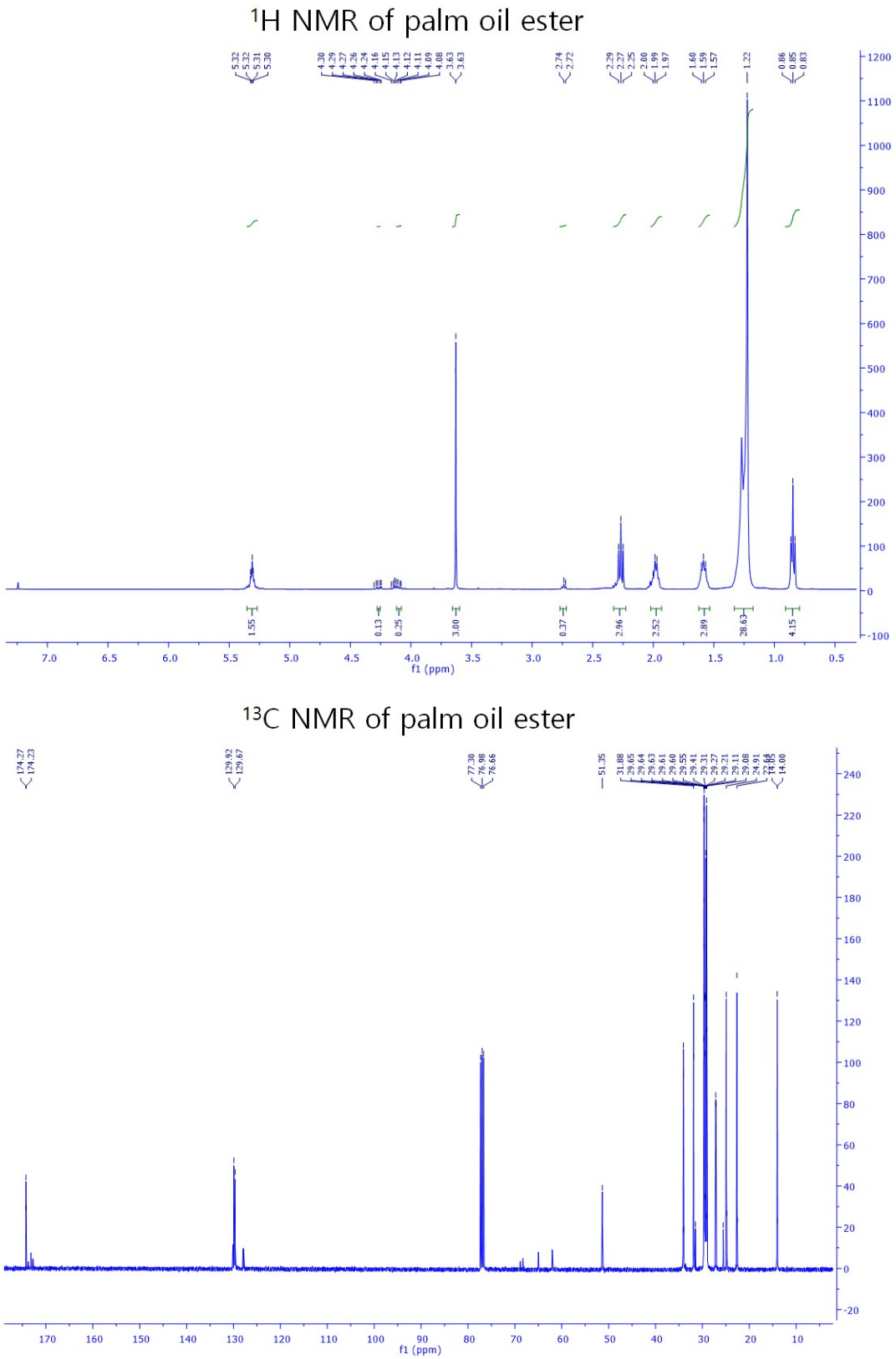

Fig. S20. [1]H and [13] C NMR spectra of palm oil ester obtained by transesterification using $OPPSO_3H$-1.

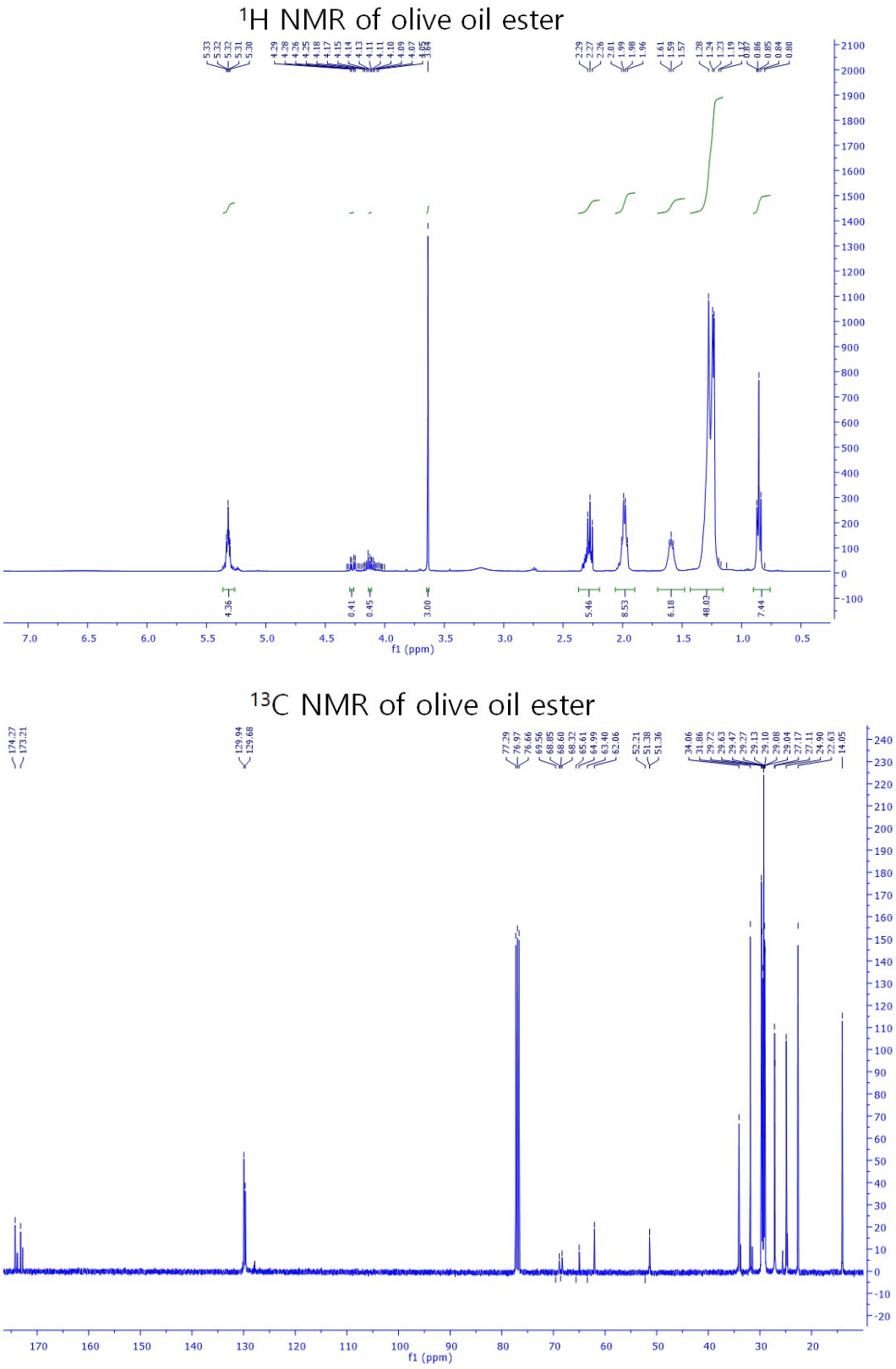

Fig. S21. [1]H and [13] C NMR spectra of olive oil ester obtained by transesterification using $OPPSO_3H$-1.